

hydroxyacyl coenzyme A dehydrogenase used for crystallization was approximately 350 μmol of NADH oxidized per min/mg of enzyme.

Crystals of L-3-hydroxyacyl coenzyme A dehydrogenase were grown in 4-ml glass vials at room temperature using a final protein concentration of 5 mg/ml. The pH of the crystallizing medium was 8.0, and it contained 0.01 M Tris, 1.0 mM EDTA, 1.0 mM dithiothreitol, and 0.05% NaN_3 . Final concentrations of polyethylene glycol were between 11 and 14% (w/v). Typically, the crystals grew to approximately 1 mm in the maximum dimension and belonged to the orthorhombic space group, C_{222} . The unit cell dimensions were $a = 227.2 \pm 0.4 \text{ \AA}$, $b = 82.2 \pm 0.2 \text{ \AA}$, and $c = 124.7 \pm 0.3 \text{ \AA}$, and the total volume of the unit cell was $2.3 \times 10^6 \text{ \AA}^3$.

To test the suitability of these crystals for x-ray analysis, a diffractometer scan of the $00l$ reflections was done and demonstrated that x-ray data to 3.0- \AA resolution could be measured. In addition, x-ray still photographs contained diffraction data extending to 2.8- \AA resolution. Generally, the crystal specimens were weakly diffracting and tended to be radiation-sensitive.

To determine the number of molecules of L-3-hydroxyacyl coenzyme A dehydrogenase/asymmetric unit, measurements of crystal density were made using a bromobenzene:xylene density gradient column calibrated with droplets of potassium phosphate, sodium chloride, and silver nitrate solutions of predetermined density (Low and Richards, 1952). The average crystal density was found to be $1.146 \pm 0.0075 \text{ g/ml}$. The density of the mother liquor (polyethylene glycol + 0.01 M Tris buffer) taken from the crystallization vials was $1.015 \pm 0.0015 \text{ g/ml}$, while the density of the Tris buffer alone was $0.9945 \pm 0.0005 \text{ g/ml}$. Using these experimentally determined values, the number of dimers of L-3-hydroxyacyl coenzyme A dehydrogenase/asymmetric unit was calculated to be approximately 1.5.

The first survey of heavy atom derivatives was carried out using crystals of the apoenzyme. While many compounds were tested in the initial survey, only PtCl_6^{2-} and methyl mercuric chloride produced detectable alterations in the x-ray diffraction pattern. These compounds also produced relatively large changes in the unit cell dimensions of the apoenzyme crystals. Specifically, the b axis changed from 82.2 to 79.6 \AA upon binding either the mercury or platinum compounds.

Because the unit cell dimension changes produced by the mercury and platinum compounds were the same, it was thought that perhaps they might be due in part to similar effects on the crystal packing. With this in mind, a series of non-heavy atom compounds was then examined to determine whether binding of these compounds would produce similar changes in the b axis. This survey of non-heavy atom compounds included 150 mM NaCl, 1.0 mM iodoacetic acid, 1.0 mM S-acetoacetyl pantetheine, and 1.0 mM NAD. With the exception of NAD, none of the compounds had any effect on the diffraction pattern. In the presence of NAD, however, detectable alterations in the x-ray pattern were observed with no significant changes in the unit cell dimensions.

Since it was not possible to prepare isomorphous heavy atom derivatives of the apoenzyme, the second survey for potential heavy atom derivatives was initiated with crystals first soaked in 1.0 mM NAD. This time, in the presence of NAD, isomorphous heavy atom derivatives could be prepared using either 0.1 mM methyl mercuric chloride, 1.0 mM PtCl_6^{2-} , or 2.0 mM IrCl_3 . Consequently, the holo-form of the crystalline enzyme was chosen as the reference system. It should be noted that the diffraction pattern of crystals soaked in 10.0 mM NAD was identical with that of crystals soaked in 1.0 mM NAD. Crystals soaked in the higher NAD concentration, however, tended to crack, and so the lower concentration was chosen for all subsequent studies. Differences between the averaged unit cell dimensions of the native crystals and the derivative crystals were always less than 1%.

X-ray Data Collection and Processing—X-ray diffraction data were collected in shells of varying 2θ ranges on a Picker four-circle diffractometer. The ranges were selected such that approximately 1000 x-ray reflections were measured per shell, which generally required one crystal. Peak intensities were calculated by a centroid peak folding procedure modified from the method described by Tickle (1975). In this approach, the centroid x of the 11-step ω -scan (0.3°) was calculated, and the peak was then taken as the sum of five steps centered around x . Slight misorientation of the reflection was corrected for by assuming a symmetrical peak. After peak intensity integration, the data were subsequently corrected for absorption, background, radiation damage, and Lorentz and polarization effects. Background estimates measured at $\pm 0.25^\circ$ in ω for 4 s were improved by averaging the values obtained from all adjacent reflections. Five different native data shells to 5.25- \AA resolution were scaled together

on the basis of 105 common reflections measured prior to the data collection run. The average agreement factor based on differences in the structure factors between the first native data set (Shell 1) and the 105 common reflections of the other shells was 3.1%. An agreement factor, again based on structure factors, between duplicate data sets of Shell 1 was 3.0%. Derivative data sets were scaled to native data sets in ranges based on $\sin \theta/\lambda$. Finally, to take into account the extra scattering contributed by heavy atoms, scale factors were calculated for each derivative by the method of Kraut *et al.* (1962). Heavy atom refinement was done independently on each shell of data.

Computational Methods—The rotation function study was carried out using the Crowther program (Crowther, 1972) and x-ray data extending from 25 to 6 \AA in resolution. The function was calculated for both the apoenzyme and the holoenzyme crystals using 5° intervals and a 35- \AA radius of integration. Out of a total 3268 unique reflections, 1327 weak reflections were omitted from the calculation. The results from the rotation function were identical for both the apo- and holoenzyme crystalline forms, and consequently only those from the holoenzyme are shown in Fig. 1. Since L-3-hydroxyacyl coenzyme A dehydrogenase is a dimeric protein, it was expected that the subunits comprising a molecule would be related by a 2-fold rotation axis. The results given in Fig. 1 correspond to κ equals 180° or 2-fold rotational symmetry, and only one significant peak was found. The importance of this finding will be discussed in a subsequent section.

Difference Patterson maps were used in the determination of heavy atom positions. One major platinum site, three major mercury sites, and two major iridium sites/asymmetric unit were located by inspection of these maps. Difference Fourier maps were calculated to confirm the positions of these heavy atom sites and to locate any minor sites. Examination of these maps revealed the location of several additional heavy atom binding sites so that in all, a total of six

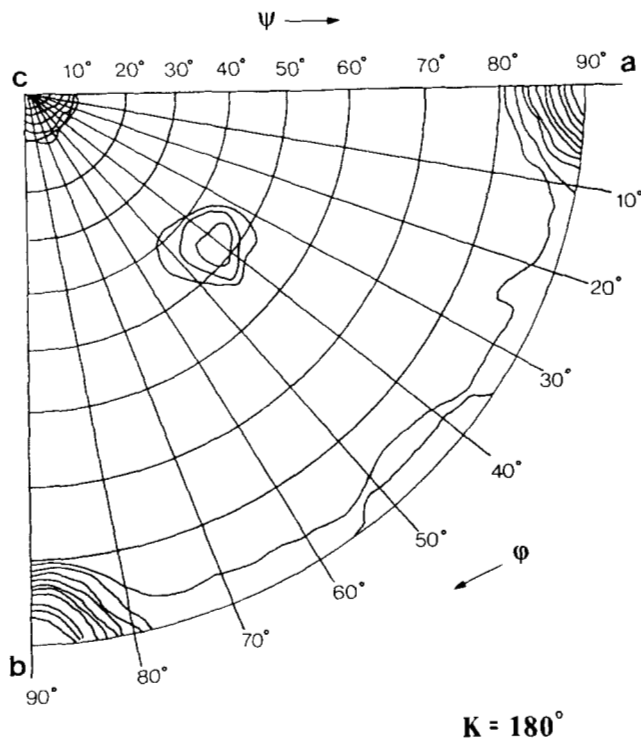


FIG. 1. Rotation function of L-3-hydroxyacyl coenzyme A dehydrogenase: κ equals 180° . The rotation function of L-3-hydroxyacyl coenzyme A dehydrogenase was calculated using the Crowther method (1972) with a native data set extending to 5.7- \AA resolution. From the map calculated at all possible Eulerian angles, those corresponding to $\kappa = 180^\circ$ were extracted and plotted as a stereographic projection using the polar angles φ and ψ . Note that because of crystallographic symmetry, only a subset of the possible angles is shown. The entire stereographic projection may be generated by envisioning 2-fold rotation operations occurring parallel to the crystallographic axes a , b , and c . As can be seen, only one principal noncrystallographic peak was observed at κ equals 180° at φ equals 45° and ψ equals 45° .

platinum sites, seven mercury sites and six iridium sites/asymmetric unit were found.

The positions and occupancies of the heavy atom sites were subsequently optimized using a refinement program written by Dr. H. Muirhead (University of Bristol, Bristol, England) which alternates successively between cycles of protein phase calculations and least squares refinement. All derivatives were used in the calculation of trial protein phases, and these phases were then used to refine the heavy atom parameters of each derivative. Refinement was carried out using shells of x-ray data corresponding to the data collection procedure and was allowed to continue until the calculated shifts in the parameters became negligible. Pertinent statistics from the refinement procedure are given in Table I. Although the IrCl_3 derivative proved useful in the initial stages of locating the heavy atom sites, it was not of much value in the final phase calculations.

The use of a coenzyme as a "heavy atom" derivative was first suggested by Sheriff and Herriott (1981) in the structural studies of ferredoxin-NADP oxidoreductase. For L-3-hydroxyacyl coenzyme A dehydrogenase, the positions of the NAD molecules were determined by difference Fourier maps using phases derived from the three heavy atom derivatives. The difference electron density map of holo- versus apo-L-3-hydroxyacyl coenzyme A dehydrogenase contained two principal coenzyme binding sites and a third site with lower occupancy (Holden *et al.*, 1981). One section of this difference map, selected because it contained electron density associated with the two principal coenzyme binding sites, is shown in Fig. 2a. The third low occupancy site is not contained in this region and was not used in the phase calculations. For both refinement and phase calculations, each NAD molecule was approximated at low resolution by a string of four "mercury" atoms spaced throughout the electron density corresponding to the bound coenzyme. Note that because the structure being determined in this study was that of the holoenzyme, the actual fourth heavy atom derivative was the apoenzyme, and thus the occupancies of the NAD pseudo-atoms were necessarily negative. The results of using the coenzyme as an additional heavy atom derivative for L-3-hydroxyacyl coenzyme A dehydrogenase were quite dramatic, as can be observed by comparing Fig. 2, b and c. Qualitatively, the molecular envelopes of the enzyme in the map phased with heavy atom derivatives and NAD were much better defined than in the map calculated with phases based only on the heavy atom derivatives. Furthermore, the electron density increased in the map which included phase information from NAD, thus indicating an improved signal to noise ratio. Quantitatively, the average figure of merit increased from 0.58 to 0.64 (5.25-Å resolution) upon inclusion of NAD in the protein phase calculations.

RESULTS AND DISCUSSION

L-3-Hydroxyacyl Coenzyme A Dehydrogenase Crystalline Packing Motif—The interpretation of the holo-L-3-hydroxyacyl coenzyme A dehydrogenase electron density map was initially complicated by the rather large amount of protein contained within the asymmetric unit, by the rather distinctive bilobal structure of the L-3-hydroxyacyl coenzyme A dehydrogenase subunit, and by the unusual manner in which the molecule packed within the unit cell. Since L-3-hydroxyacyl coenzyme A dehydrogenase is a dimer in solution, it was assumed that the asymmetric unit would contain an integral number of dimers and, based on the crystal density measure-

ments, two dimers were thought to be present.

The rotation function results shown in Fig. 1 predicted that the local dyad for each dimer was tilted at approximately $\pm 45^\circ$ with respect to all three crystallographic axes. If there were 2 dimers/asymmetric unit, their dyads would then differ only by their translational components and their polarities. In the low resolution electron density map, the local dyad for one dimer, which for discussion purposes shall be labeled Dimer 1, was readily visible. The orientation of the Dimer 1 dyad corresponded closely to the peak in the rotation function. The two major NAD binding sites and two of the major methyl mercuric chloride sites paired around this local 2-fold axis. In fact, the two mercury binding sites were used to refine the position of this dyad, and electron density maps sectioned perpendicular to this local symmetry axis contained readily visible similarities in the overall features of each subunit.

Once the bilobal nature of an individual L-3-hydroxyacyl coenzyme A dehydrogenase subunit in Dimer 1 was clearly established (see below), it then became apparent that the other molecular dyad was co-linear with the crystallographic 2-fold axis at $x = \frac{1}{2}$, $z = \frac{1}{4}$ rather than tilted at 45° . The net effect of this unique crystalline packing motif, shown schematically in Fig. 3, was to reduce the expected number of L-3-hydroxyacyl coenzyme A dehydrogenase dimers/asymmetric unit from 2.0, as originally reported, to 1.5 (Weininger and Banaszak, 1978; Holden *et al.*, 1981). Each L-3-hydroxyacyl coenzyme A dehydrogenase subunit in Fig. 3 is represented by a large and a small circle in order to emphasize the bilobal character of the low resolution structure. The molecule located in the general position and labeled *Dimer 1* in Fig. 3 is responsible for the peak on the $\kappa = 180^\circ$ section of the rotation function. The other molecule, labeled *Dimer 2* in Fig. 3, is positioned on a crystallographic 2-fold axis, and therefore its contribution to the rotation function is hidden under the large peaks arising from crystallographic symmetry. Correlation peaks between the subunits of Dimer 1 and Dimer 2 were not observed in the rotation function presumably because of the length of the intermolecular Patterson vectors generated by this packing phenomenon. With three subunits/asymmetric unit, the solvent content of the L-3-hydroxyacyl coenzyme A dehydrogenase crystals was 56% (v/v) and V_m was equal to $2.9 \text{ \AA}^3/\text{dalton}$ (Matthews, 1968).

As discussed under "Experimental Procedures," difference Fourier maps between holo- and apoenzyme crystals revealed two elongated peaks of electron density/asymmetric unit and a third peak of reduced integrated electron density near the crystallographic 2-fold axis at $x = \frac{1}{2}$, $z = \frac{1}{4}$ (Holden *et al.*, 1981). The third peak, originally believed to be noise in the difference map, actually represented low level NAD substitution at the binding sites of Dimer 2 (Holden *et al.*, 1981). It is not known if the lower NAD occupancy in Dimer 2 represents a real difference in binding affinity caused by a change

TABLE I
Heavy atom refinement

The symbols are defined as follows: d_{max} = maximum resolution of x-ray diffraction data expressed in Angstroms; $\langle F_{\text{NAT}} \rangle$, root mean square (RMS) native structure amplitude; $\langle f \rangle$, RMS calculated heavy atom amplitude; $\langle E \rangle$, RMS lack of closure error; FM , figure of merit. The number of sites are given for the asymmetric unit; there are eight equivalent positions for the space group C_{222} .

| Shell | d_{max} | $\langle F_{\text{NAT}} \rangle$ | PtCl ₃ (6 sites) | | Hg ₃ CHgCl (7 sites) | | IrCl ₃ (6 sites) | | NAD (2 sites, 8 atoms) | | FM |
|-------|------------------|----------------------------------|-----------------------------|---------------------|---------------------------------|---------------------|-----------------------------|---------------------|------------------------|---------------------|------|
| | | | $\langle f \rangle$ | $\langle E \rangle$ | $\langle f \rangle$ | $\langle E \rangle$ | $\langle f \rangle$ | $\langle E \rangle$ | $\langle f \rangle$ | $\langle E \rangle$ | |
| Å | | | | | | | | | | | |
| 1 | 8.98 | 216.0 | 31.7 | 25.5 | 34.4 | 30.8 | 19.7 | 23.3 | 38.1 | 23.0 | 0.76 |
| 2 | 7.13 | 158.0 | 19.5 | 18.7 | 30.2 | 29.8 | 10.8 | 16.0 | 25.4 | 26.3 | 0.63 |
| 3 | 6.22 | 104.0 | 13.2 | 13.7 | 20.2 | 24.7 | 8.2 | 15.7 | 19.3 | 17.5 | 0.61 |
| 4 | 5.66 | 89.9 | 12.2 | 14.0 | 23.9 | 24.4 | 4.6 | 7.9 | 17.7 | 17.1 | 0.60 |
| 5 | 5.25 | 98.1 | 12.5 | 11.9 | 17.1 | 26.6 | 6.8 | 10.1 | 18.6 | 16.7 | 0.59 |

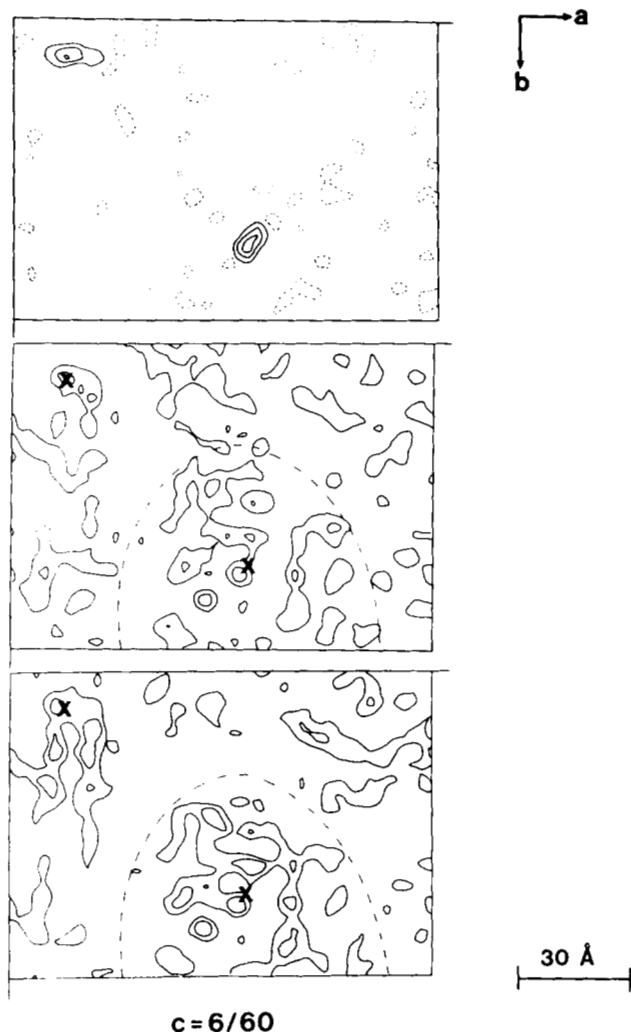


FIG. 2. The use of NAD in phasing x-ray data from L-3-hydroxyacyl coenzyme A dehydrogenase. All the drawings are of single sections of the three-dimensional electron density map perpendicular to the *c* axis and calculated with x-ray data extending to 5.25-Å resolution. *a*, one section of a difference electron density map between the holo- and apo-forms of L-3-hydroxyacyl coenzyme A dehydrogenase is shown (*top*). This section was selected because it contained peaks from the NAD bound to each of the two subunits of Dimer 1, not however in the same molecule. The numbering of the L-3-hydroxyacyl coenzyme A dehydrogenase molecules is described in the legend to Fig. 3. Negative peaks are depicted with *dashed lines* and begin at an arbitrary scale of -15, while positive electron density shown by *solid lines* begins at 15. Each new level represents an increase of 20 arbitrary units. *b*, one section of the electron density map of the holoenzyme is shown (*middle*). The map was calculated with phases obtained only with the heavy atom derivatives. The symbol *x* marks the location of the NAD site, and the *dashed line* represents the molecular envelope of Dimer 1. For the sake of clarity, only positive electron density has been contoured using about the same scale of arbitrary units described for *a*. *c*, a section of the electron density map of the holo-form of L-3-hydroxyacyl coenzyme A dehydrogenase is shown (*bottom*). X-ray phases used to calculate this map were based on the three heavy atom derivatives and two NAD binding sites. Both contouring and other symbols are the same as described for *b* and *c*.

in conformation or rather is simply a manifestation of crystalline packing.

The Low Resolution Structure of L-3-Hydroxyacyl Coenzyme A Dehydrogenase—It was anticipated that L-3-hydroxyacyl coenzyme A dehydrogenase would appear similar in structure to other NAD-dependent dehydrogenases with major differences related only to the region involved in substrate

binding. This is not the case, however. Even at 5.25-Å resolution, each L-3-hydroxyacyl coenzyme A dehydrogenase subunit displays a distinctive bilobal structure, as can be observed by studying Fig. 4, *top* and *bottom*. The molecular outline of Dimer 1, the molecule located in the general position in the unit cell, is shown in Fig. 4, *top*. It is oriented such that the molecular dyad is nearly perpendicular to the plane of the paper. Note that the drawing was obtained from an unaveraged electron density map, and yet many of the prominent features are easily visualized in both subunits. Fig. 4, *bottom*, shows the outline of one subunit of the dimer located along the crystallographic 2-fold axis. Again, the molecular dyad, and in this case the crystallographic 2-fold at $x = \frac{1}{2}$, $z = \frac{1}{4}$, is nearly perpendicular to the plane of the paper. Its overall subunit structure can be compared with the subunits of Dimer 1 shown in Fig. 4, *top*, and once again the similarities are apparent. The larger lobe of a L-3-hydroxyacyl coenzyme A dehydrogenase subunit, indicated by the letter *A*, contains the NAD binding site and has approximate dimensions of $37 \times 45 \times 35$ Å. The size of the smaller lobe, *B*, is approximately $30 \times 23 \times 20$ Å. The bilobal structure of L-3-hydroxyacyl coenzyme A dehydrogenase is somewhat unique when compared to other NAD-dependent dehydrogenases. At low resolution, a subunit of cytoplasmic malate dehydrogenase has a "bean-shaped" structure with no apparent clefts or lobes (Tsernoglou *et al.*, 1972). The same is true for the subunits of lactate dehydrogenase and of lobster, human, and *Bacillus stearothermophilus* glyceraldehyde-3-phosphate dehydrogenase (Buehner *et al.*, 1974; Watson *et al.*, 1972; Biesecker *et al.*, 1977).

Since L-3-hydroxyacyl coenzyme A dehydrogenase must have a binding site for all or part of the CoA moiety, a comparison between it and citrate synthase is also of interest. Citrate synthase catalyzes the condensation of acetyl-CoA and oxalacetic acid to form citrate. The enzyme is a dimer of subunit molecular weight equal to 44,000, and the molecular structure is known at high resolution (Remington *et al.*, 1982). In the so-called "open" conformation found in the tetragonal crystal habit, citrate synthase also has a pronounced bilobal appearance (Remington *et al.*, 1982). For citrate synthase, the AMP portion of CoA binds to the small domain, and it is reasonable to speculate that the small lobe of L-3-hydroxyacyl coenzyme A dehydrogenase may have a similar function. So far, however, it has not been possible to obtain binding of CoA to crystalline L-3-hydroxyacyl coenzyme A dehydrogenase, even at concentrations of 2 mM.

The major mercurial binding site for L-3-hydroxyacyl coenzyme A dehydrogenase occurs near the junction of the large and small lobe. Since L-3-hydroxyacyl coenzyme A dehydrogenase contains a single cysteine at position 206/309, it is likely that this residue marks the major mercurial binding site found in the heavy atom derivative studies. If it is assumed that the lobes contain contiguous segments of polypeptide chain with no crossovers between lobes and in view of the fact that NAD binding occurs in the large lobe, it is possible to speculate that the smaller segment of the protein corresponds to the COOH-terminal portion of the polypeptide chain. This folding is supported by the amino acid sequence homology of L-3-hydroxyacyl coenzyme A dehydrogenase with other dehydrogenases, suggesting that the nucleotide binding domain is found in the NH₂-terminal segment of the polypeptide chain (Bitar *et al.*, 1980).

Although not easily visible from the viewing angle shown in Fig. 4, *top* and *bottom*, some secondary structure is visible at the present resolution. For example, a rod-like segment of density fitting the dimensions of an α -helix is visible in the electron density maps. It is roughly 35-Å long and is located

FIG. 3. Schematic representation of the L-3-hydroxyacyl coenzyme A dehydrogenase crystalline packing motif. As indicated in the figure, L-3-hydroxyacyl coenzyme A dehydrogenase packs in the C_{222} unit cell with a molecule labeled *Dimer 1* in a general position and a second molecule labeled *Dimer 2* located on the crystallographic 2-fold axis at $x = \frac{1}{2}, z = \frac{1}{4}$. The orientation of the crystallographic axes is shown in the insert. The molecular dyad of *Dimer 1* is tilted at approximately 45° with respect to all three crystallographic axes. For the sake of clarity, only one out of the eight equivalent positions found in the unit cell is shown. Each L-3-hydroxyacyl coenzyme A dehydrogenase subunit in the figure is represented by a large and a small circle in order to emphasize the overall bilobal character of the enzyme.

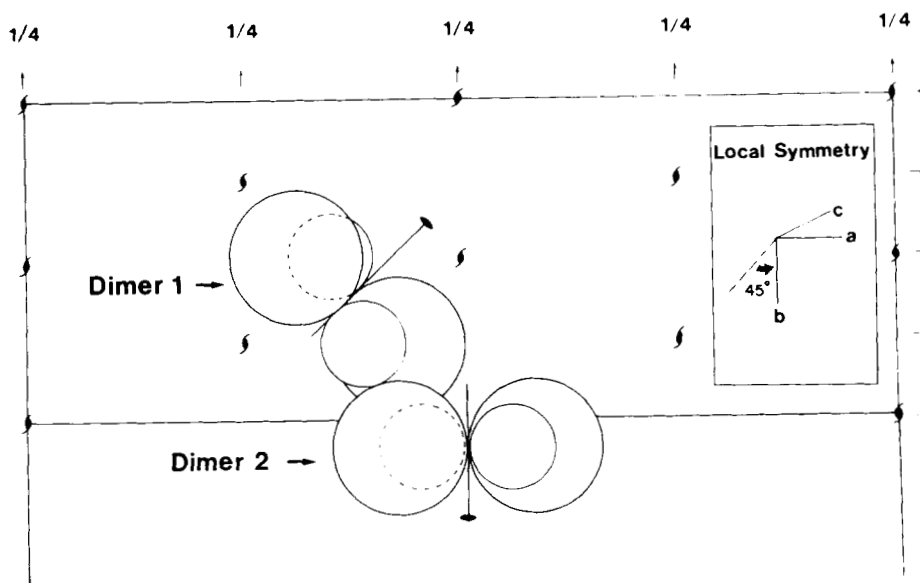
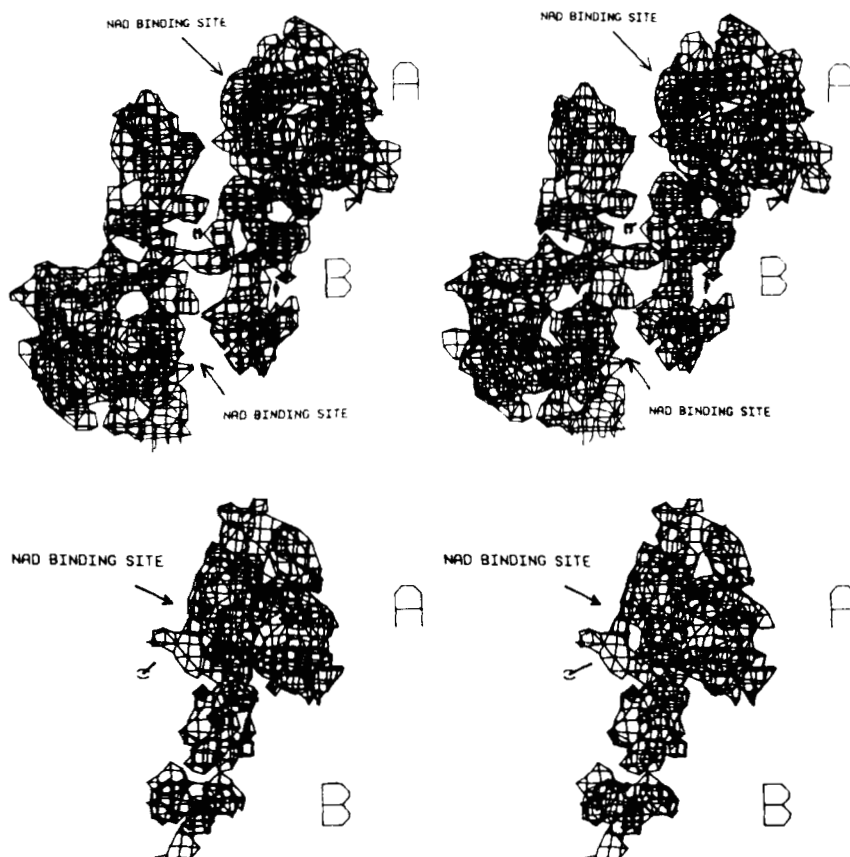


FIG. 4. The low resolution structure of L-3-hydroxyacyl coenzyme A dehydrogenase. The stereo-drawings are based on a 5.25-Å resolution electron density map and are contoured in three dimensions using an MMS-X computer graphics system. Each subunit of L-3-hydroxyacyl coenzyme A dehydrogenase contains two lobes labeled A and B. The larger lobe, A, contains the coenzyme binding site marked with an arrow. Because of the large size of the dimer, part of lobe A has been omitted from the drawing so that only about 85% of the total molecule can be seen. The 2-fold rotation axis relating the two subunits is also shown in both stereo-drawings. The molecular dyad is almost perpendicular to the plane of the drawing. *Top*, Dimer 1: the molecule of L-3-hydroxyacyl coenzyme A dehydrogenase in the general position. See Fig. 3. *Bottom*, Dimer 2: one subunit of the L-3-hydroxyacyl coenzyme A dehydrogenase molecule which is located along a crystallographic 2-fold axis. See Fig. 3.



along the outside boundary of the large lobe.

The NAD Binding Site—As can be seen in Fig. 4, top, the NAD binding sites for a given dimer are roughly 55-Å apart. This separation is considerably greater than in cytoplasmic malate dehydrogenase where they are separated by about 20 Å, thus suggesting that dimer formation may occur in a different manner for L-3-hydroxyacyl coenzyme A dehydrogenase (Webb *et al.*, 1973). Likewise, in the *B*-side-specific tetrameric enzyme glyceraldehyde-3-phosphate dehydrogenase, the NAD binding sites are separated by approximately 24.5, 38.7, and 41.6 Å, again showing no obvious correlation

with L-3-hydroxyacyl coenzyme A dehydrogenase (Buehner *et al.*, 1974; Bernstein *et al.*, 1977). It is also noteworthy that the NAD binding site occurs relatively close to the interface between the large lobe of one subunit and the small lobe of another subunit.

In all the NAD-dependent dehydrogenases studied thus far by x-ray methods, the coenzyme has been shown to bind to the protein in essentially the same open conformation with no internal interactions between the adenine and pyridine rings. In this conformation, the distance between C-2 of the nicotinamide ring and C-6 of the adenine ring is approximately 14 Å.

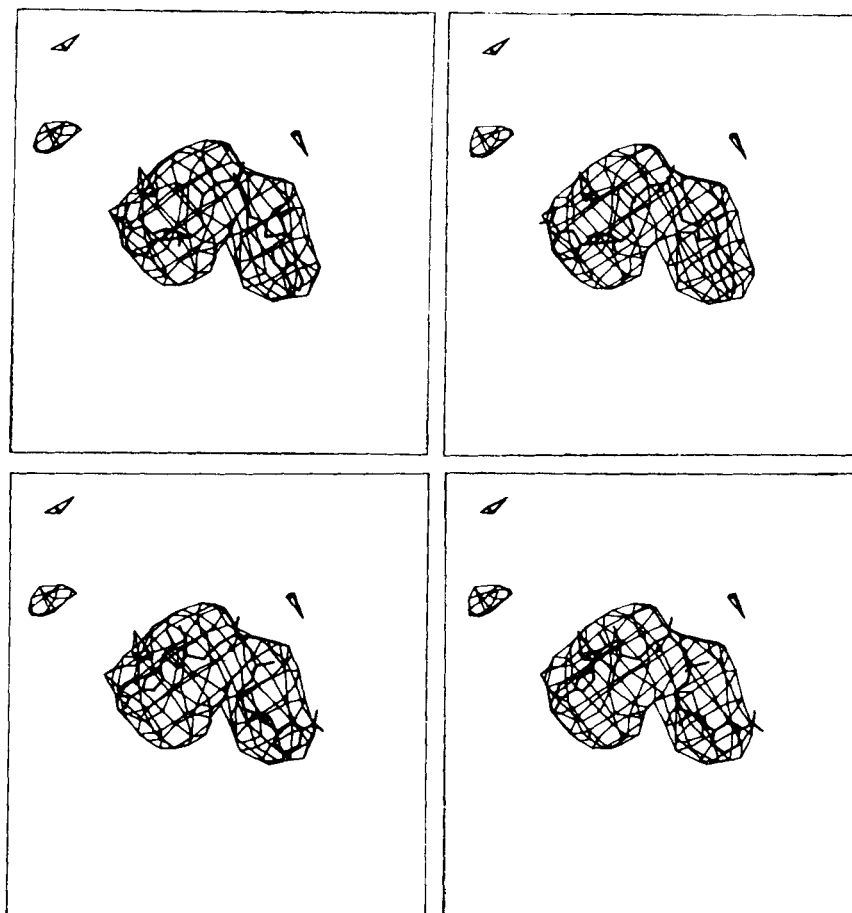


FIG. 5. NAD bound to L-3-hydroxyacyl coenzyme A dehydrogenase. The stereo-drawings show stick models of NAD in the difference electron density corresponding to a coenzyme binding site in L-3-hydroxyacyl coenzyme A dehydrogenase. The electron density shown here is associated with Dimer 1 and is located in the *rightmost* subunit in Fig. 4, *top*. The conformation of NAD is the same as that found in cytoplasmic malate dehydrogenase except that the nicotinamide ring is in the *syn*- rather than *anti*-orientation as suggested to occur in *B*-side-specific dehydrogenases. Two orientations of the NAD are possible, and they are shown in the *top* and *bottom* of the figure. At the present resolution of 5.25 Å, it is believed that the *bottom* of the figure shows the most probable configuration for reasons given in the text.

It has been suggested that the conformation of NAD when bound to "A"-side-specific dehydrogenases differs only from that of the "B"-side-specific enzymes by 180° rotation about the glycosidic bond between the nicotinamide ring and the ribose.

The difference Fourier maps calculated between crystals of the holo- and apoenzyme at 5.25-Å resolution strongly suggest that NAD also binds to L-3-hydroxyacyl coenzyme A dehydrogenase in this typical extended conformation. With this in mind, attempts to fit a molecular model of NAD to the major difference electron density peaks were carried out using the MMS-X computer graphics system. The conformation of NAD when bound to cytoplasmic malate dehydrogenase but with the nicotinamide ring rotated 180° as suggested to occur in *B*-side-specific dehydrogenases was used as the molecular model in these studies. The results are presented in Fig. 5, *top* and *bottom*. At this resolution, no attempts were made to idealize the fit of the molecular model to the difference electron density by rotating individual covalent bonds. Recalling that NAD is a dinucleotide, it should be emphasized that the adenine and nicotinamide moieties of the coenzyme will have similar features in an electron density map, especially at 5.25-Å resolution. There is thus ambiguity as to which end of the elongated peak in the difference map corresponds to the adenine group and which to the nicotinamide portion of the bound coenzyme. Independent of the aforementioned orientation ambiguity, the results shown in Fig. 5, *top* and *bottom*, demonstrate that the difference electron density found in crystalline L-3-hydroxyacyl coenzyme A dehydrogenase corresponds closely to the open conformation of NAD found in other dehydrogenases. Parenthetically, the open conformation of NAD with the nicotinamide ring rotated into the *A*-side-specific conformation fits equally well into this density. As

can be seen in Fig. 5, *top* and *bottom*, the NAD difference electron density is thicker on one end, the left-most part of the electron density in Fig. 5, *top* and *bottom*. In addition, the thinner segment of the NAD electron density is located more internal with respect to the subunit boundary. With this in mind, it is suggested that the correct orientation of NAD in the L-3-hydroxyacyl coenzyme A dehydrogenase subunit will correspond to that shown in Fig. 5, *bottom*, since it is known that the nicotinamide ring in the active site of dehydrogenases is more internal in the overall subunit structure.

In summary, L-3-hydroxyacyl coenzyme A dehydrogenase is a bilobal protein which distinguishes it from alcohol and hydroxy acid dehydrogenases. The coenzyme NAD binds in the typical open conformation and, the binding site is located relatively close to the subunit interface in this dimeric protein. The coenzyme binding site is found in the larger lobe of L-3-hydroxyacyl coenzyme A dehydrogenase, and, based on the amino acid sequence homology with other dehydrogenases (Bitar *et al.*, 1980), this lobe probably contains the NH₂-terminal segment of the polypeptide chain.

Acknowledgments—We are grateful to Tom Meininger for the preparation of crystals of L-3-hydroxyacyl coenzyme A dehydrogenase and numerous other forms of technical support. In addition, the frequent help of Dr. Richard Wrenn in maintaining an ailing diffractometer is gratefully acknowledged. We thank Dr. John McAlister for his help in the use of the MMS-X molecular graphics system. Last of all, we thank Dr. T. Blundell who, during a short discussion, aided us in recognizing the unusual packing arrangement present in this crystalline form of L-3-hydroxyacyl coenzyme A dehydrogenase.

REFERENCES

- Bernstein, F. C., Koetzle, T. F., Williams, G. J. B., Meyer, E. F., Jr., Brice, M. D., Rodgers, J. R., Kennard, O., Shimanouchi, T., and

- Tasumi, M. (1977) *J. Mol. Biol.* **112**, 535-542
- Biesecker, G., Harris, J. I., Thiery, J. C., Walker, J. E., and Wonacott, A. J. (1977) *Nature (Lond.)* **266**, 328-333
- Bitar, K. G., Perez-Aranda, A., and Bradshaw, R. A. (1980) *FEBS Lett.* **116**, 196-198
- Buehner, M., Ford, G. C., Moras, D., Olsen, K. W., and Rossmann, M. G. (1974) *J. Mol. Biol.* **90**, 25-49
- Crowther, R. A. (1972) in *The Molecular Replacement Method* (Rossmann, M. G., ed) pp. A173-178, Gordon & Breach Science Publishers, New York
- Glatthaar, B. E., Barbarash, G. R., Noyes, B. E., Banaszak, L. J., and Bradshaw, R. A. (1974) *Anal. Biochem.* **57**, 432-451
- Holden, H. M., Banaszak, L. J., Frieden, C., and McLoughlin, D. J. (1981) *FEBS Lett.* **132**, 15-18
- Kraut, J., Sieker, L. C., High, D. F., and Freer, S. T. (1962) *Proc. Natl. Acad. Sci. U. S. A.* **48**, 1417-1424
- Low, B. W., and Richards, F. M. (1952) *J. Am. Chem. Soc.* **74**, 1660-1666
- Matthews, B. W. (1968) *J. Mol. Biol.* **33**, 491-497
- Noyes, B. E., and Bradshaw, R. A. (1973a) *J. Biol. Chem.* **248**, 3052-3059
- Noyes, B. E., and Bradshaw, R. A. (1973b) *J. Biol. Chem.* **248**, 3060-3066
- Noyes, B. E., Glatthaar, B. E., Garavelli, J. S., and Bradshaw, R. A. (1974) *Proc. Natl. Acad. Sci. U. S. A.* **71**, 1334-1338
- Remington, S., Weigand, G., and Huber, R. (1982) *J. Mol. Biol.* **158**, 111-152
- Sheriff, S., and Herriott, J. R. (1981) *J. Mol. Biol.* **145**, 441-451
- Tickle, I. J. (1975) *Acta Crystallogr. Sect. B Struct. Crystallogr. Cryst. Chem.* **31**, 329-331
- Tsernoglou, D., Hill, E., and Banaszak, L. J. (1972) *J. Mol. Biol.* **69**, 75-87
- Wakil, S. J., Green, D. E., Mii, S., and Mahler, H. R. (1954) *J. Biol. Chem.* **207**, 631-638
- Watson, H. C., Duee, E., and Mercer, W. D. (1972) *Nature New Biol.* **240**, 130-133
- Webb, L. E., Hill, E. J., and Banaszak, L. J. (1973) *Biochemistry* **12**, 5101-5109
- Weininger, M. S., and Banaszak, L. J. (1978) *J. Mol. Biol.* **119**, 443-449